and solar nitrogen may result from incompletely homogenized residual heterogeneities rather than from solar system processes operating on an initially homogeneous reservoir. This suggestion is qualitatively similar to the two-component model of Geiss and Bochsler (*34*).

References and Notes

1. P. G. Wannier and M. W. Werner, in *Cosmic History of the Biogenic Elements and Compounds*, J. A. Wood and S. Chang, Eds. (NASA SP-476, Washington, D.C., 1985), pp. 11–19.
2. S. Starrfield, J. W. Truran, W. M. Sparks, G. S. Kutter, *Astrophys. J.* **176**, 169 (1972).
3. W. M. Howard, W. D. Arnett, D. D. Clayton, *ibid.* **165**, 495 (1971).
4. J. Audouze *et al.*, in *CNO Isotopes in Astrophysics*, J. Audouze, Ed. (Reidel, Dordrecht, 1977), pp. 155–171.
5. D. D. Clayton, *Astrophys. J.* **280**, 144 (1984).
6. Nitrogen isotope ratios are expressed in δ notation: δ (per mil) = $(R_{sample}/R_{reference} - 1)$ 1000, where $R = {}^{15}N:{}^{14}N$. The reference is AIR (atmospheric nitrogen). Carbon isotope ratios are given as $\delta^{13}C$ relative to the PDB (Peedee Belemnite) standard.
7. C. A. Prombo and R. N. Clayton, *Meteoritics* **18**, 377 (1983).
8. F. Robert and S. Epstein, *Geochim. Cosmochim. Acta* **46**, 81 (1982).
9. C. C. Kung and R. N. Clayton, *Earth Planet. Sci. Lett.* **38**, 421 (1978).
10. R. S. Lewis, E. Anders, I. P. Wright, S. J. Norris, C. T. Pillinger, *Nature (London)* **305**, 767 (1983).
11. J. Halbout, T. K. Mayeda, R. N. Clayton, *Lunar Planet. Sci.* **16**, 314 (1985).
12. J. F. Kerridge, *Earth Planet. Sci. Lett.* **64**, 186 (1983).
13. ———, *Geochim. Cosmochim. Acta* **49**, 1707 (1985).
14. J. F. Lovering, in *Researches on Meteorites*, C. B. Moore, Ed. (Wiley, New York, 1962), p. 179; G. W. Kallemeyn, W. V. Boynton, J. Willis, J. T. Wasson, *Geochim. Cosmochim. Acta* **42**, 507 (1978).
15. H. E. Newsom and M. J. Drake, *Geochim. Cosmochim. Acta* **43**, 689 (1979).
16. B. Mason and J. Nelen, *ibid.* **32**, 661 (1968).
17. R. N. Clayton and T. K. Mayeda, *Earth Planet. Sci. Lett.* **40**, 168 (1978).
18. Each result in Table 1 is the product of a single nitrogen extraction and isotopic analysis. The errors quoted for $\delta^{15}N$ are the statistical errors (1σ) in the mass spectrometry only. Heterogeneity in the meteorite is indicated by differences in nitrogen contents and isotopic composition between clast 1 and clast 2. In the normal procedure for isotope ratio measurement with the Micromass 602C spectrometer, the ion beams $^{14}N^{14}N^+$ and $^{14}N^{15}N^+$ are collected simultaneously, and their ratio is compared with that for a N_2 reference gas. In the present work, the sample ratios were beyond the range of the instrument, so that modified procedures were required. In particular, the values for "Whole rock" in Table 1 were determined by a single-beam method, in which *m/e* values of 28 and 29 were measured separately, and then $\delta^{15}N$ was calculated. This procedure results in poorer precision. Verification that the large excesses at *m/e* = 29 were due to $^{14}N^{15}N^+$ ions rather than an isobaric contamination was accomplished in two ways. First, the gas samples were recycled through the chemical purification procedure to ensure complete oxidation and removal of hydrocarbons and carbon monoxide. Second, the intensity of the ion beam at *m/e* = 30 was measured (in two different mass spectrometers) and found to be exactly that expected for $^{15}N^{15}N^+$ calculated on the basis of the ratio of *m/e* = 29 to *m/e* = 28. That similar nitrogen contents and isotopic compositions were found for two meteorites that fell on opposite sides of Earth (Australia and the United States) proves that the results are properties of the meteorite parent body, not the consequence of any terrestrial alteration process.
19. E. S. Simpson and D. G. Murray, *Mineral. Mag.* **23**, 33 (1932).
20. L. Grossman, E. Olsen, J. T. Lattimer, *Science* **206**, 449 (1979).
21. R. N. Clayton and T. K. Mayeda, *Earth Planet. Sci. Lett.* **67**, 151 (1984).
22. M. Arnould and H. Norgaard, *Astron. Astrophys.* **64**, 195 (1978).
23. P. K. Swart, M. M. Grady, C. T. Pillinger, R. S. Lewis, E. Anders, *Science* **220**, 406 (1983).
24. J. Yang and S. Epstein, *Nature (London)* **311**, 544 (1984).
25. D. D. Clayton, E. Dwek, S. E. Woosley, *Astrophys. J.* **214**, 300 (1977).
26. N. G. Basov *et al.*, *Sov. Phys. Uspekhi* **20**, 209 (1977).
27. T. J. Manuccia and M. D. Clark, *Appl. Phys. Lett.* **28**, 372 (1976).
28. N. G. Adams and D. Smith, *Astrophys. J.* **247**, L123 (1981).
29. T. Owen *et al.*, *J. Geophys. Res.* **82**, 4635 (1977).
30. F. Begemann, H. W. Weber, E. Vilcsek, H. Hintenberger, *Geochim. Cosmochim. Acta* **40**, 353 (1976).
31. H. Stauffer, *J. Geophys. Res.* **67**, 2023 (1962).
32. I. A. Franchi, D. W. McGarvie, I. P. Wright, C. T. Pillinger, in *Abstracts of the 48th Meeting of the Meteoritical Society*, Bordeaux, France, 16 to 19 July 1985.
33. F. A. Podosek, *Annu. Rev. Astron. Astrophys.* **16**, 293 (1978).
34. J. Geiss and P. Bochsler, *Geochim. Cosmochim. Acta* **46**, 529 (1982).

35. We thank R. S. Clarke for providing a slice of Bencubbin, D. C. Zhang for analyzing Weatherford, and T. K. Mayeda for valuable assistance with the mass spectrometry. Supported by NASA grant NAG 9-51.

12 July 1985; accepted 23 September 1985

Crystal Axes in Recent and Fossil Adult Echinoids Indicate Trophic Mode in Larval Development

Abstract. *The type of larval development in echinoids (Phylum Echinodermata) was found to determine crystal patterns in adult apical skeletal plates. This relation between larvae and adults will allow fossil species to be examined to determine the effects of developmental mode on evolutionary patterns, such as species longevity and speciation rate. Independent tests of hypotheses of such patterns now shown among fossil mollusks with and without feeding larvae can thus be performed.*

RICHARD B. EMLET*
Department of Zoology and
Friday Harbor Laboratories,
University of Washington,
Seattle 98195

*Present address: Department of Invertebrate Zoology, Natural History Museum, Smithsonian Institution, Washington, D.C. 20560.

Developmental mode has been linked to geographic distribution, species longevity, and speciation rate in benthic marine organisms (*1*). This connection is based on a varying opportunity for dispersal, and contrasts species having long-lived, planktonic, feeding larvae that can disperse over great distances with species having nonfeeding larvae that develop more quickly and have limited or no dispersal. Species with feeding larvae are predicted to be geographically widely distributed and geologically long-lived and to speciate infrequently. Species with nonfeeding larvae are predicted to be geographically narrowly distributed, geologically short-lived, and prone to speciation and extinction events (*1, 2*). These predictions are supported by patterns among fossil gastropod mollusks (*3*). To date, developmental mode has been inferred for gastropods and bivalves because adult shells include a larval shell that indicates the mode of larval development (*4*).

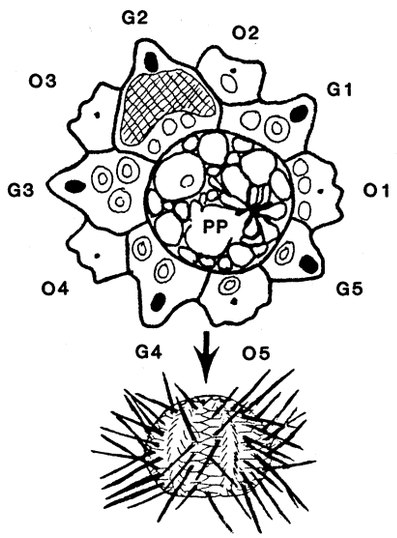

Fig. 1. Camera lucida drawing of the apical system of an echinoid. Five genital (G) and five ocular (O) plates surround the periproct (PP). The arrow indicates the location of the apical system on the aboral surface of an adult echinoid.

Here I show that type of larval development can be inferred from Recent and fossil adult skeletons in another taxon, the echinoderm class Echinoidea, from crystal orientations in adult apical plates (Fig. 1). Echinoid larvae have skeletal rods and postmetamorphic juveniles have skeletal plates, but crystal axes of the rods determine crystal axes of some of the plates.

The echinopluteus larva of echinoids (Fig. 2A) feeds and swims with a ciliated band on epidermal projections called arms (*5*). Each arm contains a skeletal rod composed of calcite, like adult spines and test plates. Each rod behaves optically like a single crystal (*6*). In species with nonfeeding larvae, the pluteus form does not develop; the larvae lack arms, rods, an elaborate ciliated band, and a larval gut (*7, 8*).

Rearrangement of the pluteus at metamorphosis leaves the larval rods on the aboral surface of the settled juvenile.

Table 1. Site of origin of ten apical plates [five genital (G) and five ocular (O)] of echinoids (*10, 11*). Larval arm and rod terminology is that of Mortensen (*7*).

Apical plate	Site of formation in	
	Feeding larva	Nonfeeding larva
G1	De novo	De novo
G2 (madreporite)	Dorsal arch rod	De novo
G3	Right posterodorsal rod	De novo
G4	Posterior transverse rod	De novo
G5	Right postoral rod	De novo
O1	De novo	De novo
O2	De novo	De novo
O3	De novo	De novo
O4	Left posterodorsal rod	De novo
O5	Left postoral rod	De novo

Table 2. Orientation of optic axes for larval rods and genital plates of five species of echinoids: *Strongylocentrotus droebachiensis* (*S.d.*); *S. franciscanus* (*S.f.*); *Echinometra vanbrunti* (*E.v.*); *Arbacia stellata* (*A.s.*); and *Dendraster excentricus* (*D.e.*). Optic axis orientations are given relative to long axis of rods and planar surface of plates (∥, parallel; ⊥, perpendicular; and ND, no data).

	S.d.	*S.f.*	*E.v.*	*A.s.*	*D.e.*
	Larval rods				
Postoral spicules	∥	∥	∥	∥	∥
Posterodorsal spicules	∥	∥	∥	∥	∥
Dorsal arch spicule	⊥	⊥	⊥	⊥	⊥
Posterior transverse spicule (*24*)	∥	∥	∥	ND	∥
	Genital plates				
G1	⊥	⊥	⊥	⊥	ND
G2	⊥	⊥	⊥	⊥	⊥
G3	∥	∥	∥	ND	ND
G4	⊥	⊥	⊥	ND	ND
G5	∥	∥	∥	ND	ND

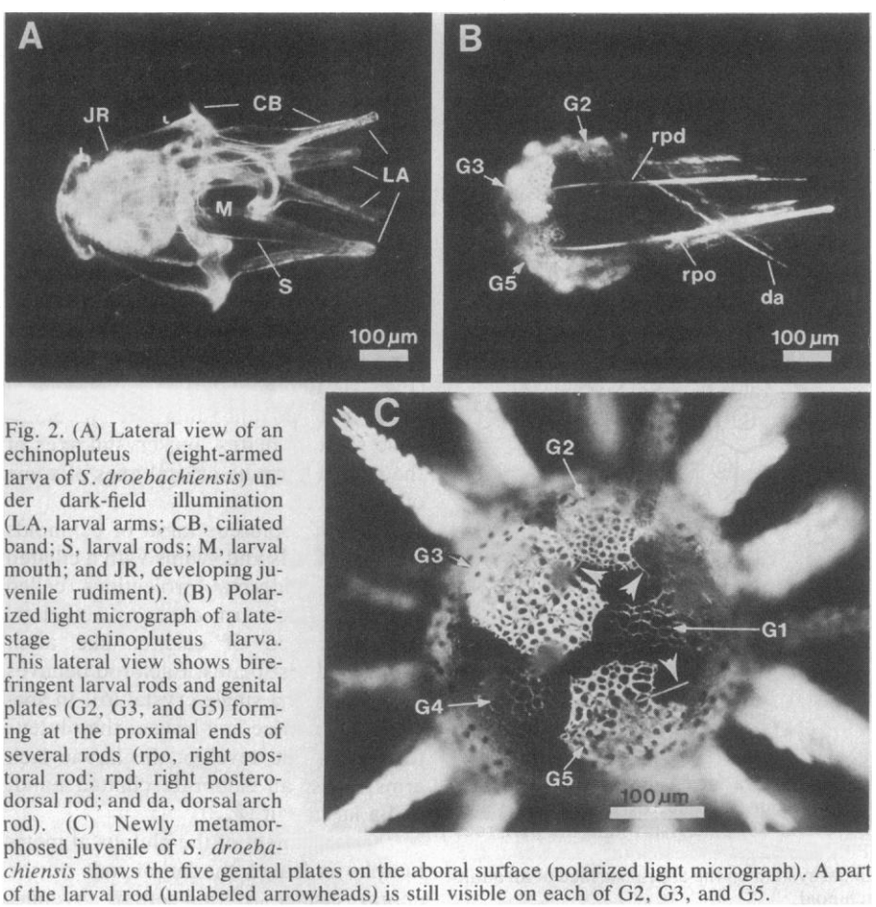

Fig. 2. (A) Lateral view of an echinopluteus (eight-armed larva of *S. droebachiensis*) under dark-field illumination (LA, larval arms; CB, ciliated band; S, larval rods; M, larval mouth; and JR, developing juvenile rudiment). (B) Polarized light micrograph of a late-stage echinopluteus larva. This lateral view shows birefringent larval rods and genital plates (G2, G3, and G5) forming at the proximal ends of several rods (rpo, right postoral rod; rpd, right posterodorsal rod; and da, dorsal arch rod). (C) Newly metamorphosed juvenile of *S. droebachiensis* shows the five genital plates on the aboral surface (polarized light micrograph). A part of the larval rod (unlabeled arrowheads) is still visible on each of G2, G3, and G5.

Larval epidermal tissue retracts from the rods and their distal tips are cut off (*9*). Despite this major rearrangement of the body, the plan of the larval body remains encoded in the apical plates because the larval rods influence the optic axes (crystallographic or C-axes) of the crystalline apical plates (Fig 2, B and C). Studies of the skeletal development of echinoids show that six of the ten apical plates grow from the proximal ends of larval rods (Table 1 and Fig. 2B) (*10, 11*). The four other apical plates in species with feeding larvae and apparently all ten apical plates in species with nonfeeding larvae form de novo during formation of the echinus (juvenile) rudiment (*7, 8, 10, 11*).

In species with feeding larvae, each of six apical plates grows out of a larval rod at an angle determined by the angle the rod makes with the developing juvenile rudiment and the pattern of growth of the new plate. Okazaki and Inoue (*6*) showed that most larval rods have an optic axis that is aligned with the long axis of the larval rod. My own observations extend and qualify this result. A plate that begins as an elaboration of a larval rod has a C-axis parallel to the C-axis of the rod from which the plate starts. Thus, a plate that grows parallel to the rod should have an optic axis in the plane of the plate surface. A plate that grows at an angle to the long axis of the larval rod should have a C-axis inclined to the plate surface. The dorsal arch rod is exceptional in having the C-axis perpendicular to the long axis of the skeletal rod, and this difference is reflected in the skeletal plate (G2) formed from it.

A petrographic microscope fitted with a Universal stage was used to determine optic axes of the larval rods and the genital plates in late-stage larvae of *Strongylocentrotus droebachiensis*, *Strongylocentrotus franciscanus*, *Echinometra vanbrunti*, *Arbacia stellata*, and *Dendraster excentricus*. C-axis orientations of the genital plates (G1 to G5) were also determined for newly metamorphosed juveniles of *S. droebachiensis*, *S. franciscanus*, and *E. vanbrunti* (*12*). The following patterns emerged (Table 2):

1) In all species observed except *D. excentricus* (*13*), G1 forms de novo and has a C-axis perpendicular to the plate surface (*14*).

2) In all species the dorsal arch rod has a C-axis that is perpendicular to the long axis of the rod. The madreporite plate (G2) that forms in the plane of this rod has a C-axis that is perpendicular to the plate surface.

3) The posterior transverse rod has a C-axis parallel to the anterior-posterior (A–P) axis of the larval body. G4 forms at the base of this rod but grows in a plane perpendicular to the A–P axis. G4 has a C-axis coincident with that of the posterior transverse rod and thus perpendicular to the plate surface.

4) In all species examined, the right posterodorsal and right postoral rods (which give rise to G3 and G5, respectively) have C-axes parallel to the rod axes. In *S. droebachiensis*, *S. franciscanus*, and *E. vanbrunti*, G3 and G5 form in planes parallel to the lengths of the rods and have C-axes parallel to the plate surfaces (*15*).

The C-axis patterns observed in newly metamorphosed juveniles are in agreement with observations of larvae competent to metamorphose. G3 and G5 have C-axes in the plane or at low angles to the plane of the apical system. G1, G2, and G4 have optic axes ~30° off the juvenile aboral-oral axis but close to perpendicular to their respective plate surfaces (Table 2). The optic axes of the last three plates are not perpendicular to the apical system as they are in adults because the plates of the apical system are domed (that is, all plates are not yet coplanar) in the early juvenile stage.

Apical plates G3 and G5 are the key to the developmental mode. A feeding larva is indicated if the C-axis orientation in each of these plates departs considerably from perpendicular to the plate surface and if their C-axis orientations differ from the C-axis orientations of G1, G2, and G4.

In a systematic study, Raup (*16*) determined the orientation of C-axes in adult apical plates of 85 extant species of echinoids and presented evidence for familial "signatures" in crystallographic patterns. He remarked that "crystal orientations in the adult apical system may be fixed in the earliest stages of development of the echinus rudiment" (*16*, p. 949). Raup also provided preliminary evidence that departures from typical family patterns occur in species with large yolky eggs by noting eight species that were exceptions to family patterns. A search of published information on these eight species shows that one develops from large yolky eggs into a nonfeeding larva and that three others produce large yolky eggs; no information is available on the remaining four species (*17*). Of the remaining 73 nonechinothuriid species (*18*) that fit the respective family patterns, 41 are known to produce feeding larvae and 6 produce small eggs that probably develop into feeding larvae. No information is available for 26 others (*17*). No species that fit family patterns are known to produce nonfeeding larvae and no exceptions to family patterns are known to produce feeding larvae. All eight of Raup's exceptions to family patterns have genital plates (G1 to G5) with similar C-axes that are nearly perpendicular to plate surfaces. Within a family, the angle that the optic axis forms with the plate surface of G3 and G5 is always higher in species with nonfeeding larval development than in species with feeding larval development. Raup's extensive survey of apical systems thus supports the observations on plate formation and optical axes of larval rods.

Some irregular echinoids (for example, heart urchins, Order Spatangoida) in which the anus has moved out of the apical system should also lend themselves to inference of developmental mode. For spatangoids, and several fossil species in their stem group, disasteroids, Jesionek-Szymanska (*19*) used optic axis patterns to identify G5, the plate that migrates with the periproct out of the apical system. Her data also showed that the optic axis of G3 has a characteristically low angle with the plate surface in an extant species with feeding larvae. A comparison with species that have nonfeeding larvae has not been made.

Until now, inference of developmental mode in echinoids has been limited to examination of gonopores (*20*) or to those brooding species that contain a depression called a marsupium in the test (*21*). Not all brooders have a marsupium (*21*). The gonopore method, unlike the apical system analysis, is sensitive to sexual dimorphism and requires larger samples for analysis of statistical differences.

Echinoids are the only class of extant echinoderms in which the apical plates grow from the larval skeleton. Crinoids, asteroids, and holothurioids do not have a larval skeleton of calcareous rods. Ophiuroids possess a well-developed larval skeleton, but juvenile plates develop independently of this larval skeleton (*22*). These differences among classes in the origin of the juvenile plates suggest that the method for echinoids cannot be extended to other classes of extant echinoderms.

Echinoids, especially the irregular forms, such as spatangoids, have a good fossil record (*23*). Analysis of the apical system is easily applied to museum specimens and indicates the type of larval development. The type of larval development indicates duration of the planktonic period and hence the capacity for dispersal. Determination of developmental mode in fossil echinoids will test the generality of biogeographic and evolutionary patterns now being established for molluskan species with and without feeding larvae (*3*).

References and Notes

1. T. Shuto, *Lethaia* **7**, 239 (1974); R. S. Scheltema, in *Concepts and Methods of Biostratigraphy*, E. G. Kauffman and J. E. Hazel, Eds. (Dowden, Hutchinson & Ross, Stroudsburg, Pa., 1977), pp. 73–108; in *Marine Organisms*, B. Battaglia and J. A. Beardmore, Eds. (Plenum, New York, 1978), pp. 303–322.
2. D. Jablonski and R. A. Lutz, *Biol. Rev.* **58**, 21 (1983).
3. T. A. Hansen, *Science* **199**, 885 (1978); *Paleobiology* **6**, 193 (1980); D. Jablonski, in *Third North American Paleontological Convention Proceedings*, B. Mamet and M. J. Copeland, Eds. (Montreal, Canada, 1982), vol. 1, pp. 257–262; T. A. Hansen, *Science* **220**, 501 (1983).
4. G. Thorson, *Biol. Rev.* **25**, 1 (1950); D. Jablonski and R. A. Lutz, in *Skeletal Growth of Aquatic Organisms*, D. C. Rhoads and R. A. Lutz, Eds. (Plenum, New York, 1980), pp. 323–377.
5. R. R. Strathmann, *J. Exp. Mar. Biol. Ecol.* **6**, 109 (1971); *Am. Zool.* **15**, 717 (1975).
6. K. Okazaki and S. Inoue, *Dev. Growth Diff.* **18**, 413 (1976).
7. T. Mortensen, *Studies on the Development and Larval Forms of Echinoderms* (Gad, Copenhagen, 1921).
8. D. H. C. Williams and D. T. Anderson, *Aust. J. Zool.* **23**, 371 (1975); S. Amemiya and T. Tsuchiya, *Mar. Biol.* **52**, 93 (1979).
9. H. Bury, *Q. J. Microsc. Sci.* **38**, 45 (1895); K. Onoda, *Mem. Coll. Sci. Kyoto Imp. Univ.* **7**, 103 (1931).
10. I. Gordon, *Philos. Trans. R. Soc. London Ser. B* **214**, 259 (1926); *ibid.* **215**, 255 (1926); K. Onoda, *Jpn. J. Zool.* **6**, 637 (1936).
11. I. Gordon, *Philos. Trans. R. Soc. London Ser. B* **217**, 289 (1929).
12. Echinoderm calcite behaves optically like a uniaxial crystal and has strong birefringence. C-axis orientation with respect to long axes of larval rods, genital plate surfaces, and apical system planes was determined on calcite structures by the methods of R. C. Emmons [*Geol. Soc. Am. Mem. 8* (1943)]. Preserved intact specimens of late-stage larvae and newly metamorphosed juveniles were mounted in Canada balsam.
13. In the clypeasteroid *Dendraster excentricus* only G2 forms before metamorphosis. Feeding larvae of clypeasteroids, perhaps because they have only a single genital plate (G2) as adults, do not show the same elaboration of other larval rods before metamorphosis (*11*).
14. Gordon (*11*) stated that G1 formed from the right anterolateral spicule in *Arbacia punctulata* and noted that, in mounted specimens, the larval rod was "broken across just above the genital 1" (p. 293). My own observations of the closely related *A. stellata* show that this larval rod abuts the forming G1 plate, but that their respective C-axis orientations differ by ~90°, a difference too great to have occurred by breakage. This difference in crystal orientation indicates that these adjacent structures form separately. Gordon's work was done without the aid of polarized light, so she could not see the C-axis pattern that contradicts her hypothesis of breakage.
15. In my specimens of *A. stellata*, regions on the distal ends of the spicules where G3 and G5 were going to form were not yet clear at the time of preservation. For *D. excentricus* see (*13*).
16. D. M. Raup, *J. Paleontol.* **39**, 934 (1965).
17. R. B. Emlet, L. R. McEdward, R. R. Strathmann, in *Echinoderm Studies II*, M. Jangoux and J. M. Lawrence, Eds. (Balkema, Rotterdam, in press).
18. Table 2 of Raup (*16*) shows the family-specific, C-axis orientations of the different genital plates. In his table the Echinothuriidae, which are known to produce only large yolky eggs, show a pattern that would be expected of feeding larvae. Reexamination of the data shows that only one of the four species examined by Raup has the pattern for larval feeding, and there is no reproductive information available for this species, *Araeosoma belli*. The other three species examined by Raup are all known to produce large yolky eggs and do not show the pattern for larval feeding.
19. W. Jesionek-Szymanska, *Acta Palaeon. Pol.* **4**, 339 (1959).
20. T. Mortensen, *Monograph of the Echinoidea I–V* (Reitzel, Copenhagen, 1928–1951); A. H. Müller, *Dtsch. Akad. Wiss. Berlin Monatsber.*

12, 923 (1970). Mortensen adopted gonopore size as an indication of developmental mode, but there is no thorough investigation of its validity. In principle, small gonopores must indicate small eggs (or a male), but large gonopores do not necessarily imply large eggs.
21. P. Kier, in *Sexual Dimorphism in Fossil Metazoa and Taxonomic Implications*, G. E. G. Westermann, Ed. (Schweizerbart'sche Verlag, Stuttgart, West Germany, 1969), pp. 215–221; G. M. Philip and R. J. Foster, *Paleontology* **14**, 666 (1971).
22. H. Ludwig, *Z. Wiss. Zool.* **36** (1881); S. Murakami, *Annot. Zool. Jpn.* **16**, 135 (1937).
23. P. M. Kier, *Paleobiology* **3**, 168 (1977); A. B. Smith, *Echinoid Palaeobiology* (Allen & Unwin, London, 1984).
24. This rod has different shapes in different species. In all species, part of the rod runs transverse to the A–P axis of the larval body. The optic axis orientation is given relative the A–P axis of the larval body.
25. I thank D. Raup for kindly allowing me to reexamine his data on apical system crystallography. I am also grateful to D. Cowen for making the Universal stage microscope available; to R. Haugerud for instruction in its use; and to A. Kohn, P. Mace, D. Raup, and R. Strathmann for comments on the manuscript. Supported by NSF grant OCE-8400818 to R. Strathmann and by a 10-week graduate student fellowship from the Smithsonian Institution.

31 May 1985; accepted 30 August 1985

Assignment of the Gene for Myelin Proteolipid Protein to the X Chromosome: Implications for X-Linked Myelin Disorders

Abstract. *Several inherited disorders in humans and in rodents result in myelin dysgenesis and a deficiency of the molecular constituents of myelin. A complementary DNA to one of the two major myelin proteins, myelin proteolipid protein (also known as lipophilin), has been used with Southern blot analysis of somatic cell hybrid DNA to map the human proteolipid protein gene to the middle of the long arm of the human X chromosome (bands Xq13-Xq22) and to assign the murine proteolipid protein gene to the mouse X chromosome. Comparison of the gene maps of the human and mouse X chromosomes suggests that myelin proteolipid protein may be involved in X-linked mutations at the mouse jimpy locus and has implications for Pelizaeus-Merzbacher disease, a human inherited X-linked myelin disorder.*

HUNTINGTON F. WILLARD
Department of Medical Genetics, University of Toronto, Toronto, Ontario M5S 1A8, Canada
JOHN R. RIORDAN
Research Institute, Hospital for Sick Children, Toronto, Ontario M5G 1X8, and *Departments of Biochemistry* and *Clinical Biochemistry, University of Toronto*

The myelin of the central nervous system (CNS) contains two major membrane proteins, myelin basic protein (MBP) and proteolipid protein (PLP) (also known as lipophilin) (1). The structural role of these proteins in the maintenance of myelin function has been elucidated by extensive biochemical analysis of the purified proteins (*2*). Humans and other mammals are subject to a number of genetically determined demyelinating diseases that occur when one or both of these constituent proteins is deficient (*3*). In mutant mice homozygous for the *shiverer* mutation, the CNS myelin is depleted of MBP as the result of a partial deletion of the autosomal MBP gene; thus genetic defects at the MBP locus can have extreme effects on myelin formation and central nervous system function (*4*). Genetic analyses of the role of PLP in the central nervous system became possible recently, with the molecular cloning and characterization of a complementary DNA (cDNA) for bovine PLP (*5*). As an initial step in such studies, we have used the PLP cDNA to assign the PLP gene to the X chromosome in both man and mouse. In addition, we have localized this gene to the middle of the long arm of the human X chromosome. Comparison of the gene maps of the mouse and human X chromosomes suggests that the PLP gene may have a primary role in several X-linked inherited myelin disorders.

Southern blotting experiments were performed with a ^{32}P-labeled cDNA (pLP1), containing a 0.95–kilobase pair (kbp) insert fragment that includes 444 base pairs of coding sequence corresponding to the carboxyl terminal half of lipophilin and about 500 base pairs of 3′ untranslated sequence (*5*). When hybridized to nitrocellulose filters containing genomic human DNA digested with Eco RI, the PLP cDNA detects two hybridizing bands of lengths 9.0 kbp and 1.3 kbp (Fig. 1). When DNA's were examined from individuals with different numbers of X chromosomes, the hybridization signals of both bands varied in a dose-dependent fashion (Fig. 1, lanes 1, 2, and 3). Thus, the bands detected in DNA from a normal 46,XX female (lane 1) were approximately twice as intense as bands observed in the same amount of DNA from a normal 46,XY male (lane 2). Bands detected in DNA from a 49,XXXXX female were substantially more intense (lane 3). These data suggest that human PLP gene sequences are confined to the X chromosome, since autosomal DNA sequences would be present in identical doses in the three DNA samples.

The chromosomal assignment of the PLP gene made by dosage was confirmed by Southern blot analysis of DNA extracted from 18 human × mouse or human × Chinese hamster somatic cell hybrids, prepared and characterized as described previously (*6*). The ^{32}P-labeled lipophilin cDNA was hybridized to Eco RI–digested DNA from the hybrid lines and from normal mouse and Chinese hamster cells. The two human DNA bands could easily be distinguished from single bands observed either in mouse DNA (8.5 kb) (Fig. 1, lane 4) or in Chinese hamster DNA (20 kb) (Fig. 1, lane 8). Both human DNA bands were present in hybrids containing a normal human X chromosome (Fig. 1, lanes 5, 6, 12, and 13) and absent from hybrids lacking this chromosome (Fig. 1, lane 7). Table 1 summarizes the complete data and the chromosomal content of the 18 hybrids. The X chromosome was the only chromosome with no discordancies; all other human chromosomes were discordant in at least 8 (44 percent) of the 18 hybrids. Hybrids AHA-llaB1 and cl 2D contain the human PLP gene and have a human X chromosome as their only identifiable human material (*7*). In addition, the hybrid pair, A54-8A (which contains the human PLP gene) and A54-8AAz22 (which does not), provide direct evidence for X-linkage of the PLP gene, since they differ only by the absence of the X chromosome from A54-8AAz22, which was derived from A54-8A by back-selection in medium containing 8-azaguanine to select cells that had lost an X chromosome (*6*, *8*).

Four of the hybrids examined contain only portions of the human X chromosome as a result of X;autosome translocations in the human cells used to prepare the hybrids. Examination of DNA from these hybrids provided information on the regional localization of the PLP gene on the X chromosome. PLP gene sequences were present in a hybrid containing the distal two-thirds of the long arm of the X (Xq13-Xqter) (Fig. 1, lane 11), and absent from hybrids containing the entire short arm of the X, the short arm and the proximal third of the long arm (Xpter-Xq13) (Fig. 1, lane 9), or the distal half of the long arm (Xq22-qter) (Fig. 1, lane 10). Thus, PLP sequences can be localized to region Xq13-Xq22, in the middle of the long arm of the human X chromosome.